J. Fluid Mech. (1978), *vol.* 87, *part* 1, *pp.* 85–96
Printed in Great Britain

Drag on a sphere in unsteady motion in a liquid at rest

By S. K. KARANFILIAN AND T. J. KOTAS
Department of Mechanical Engineering, Queen Mary College, Mile End Road, London E1 4NS

(Received 10 December 1976 and in revised form 7 October 1977)

A sphere was subjected to a simple harmonic motion in an otherwise undisturbed liquid. Records of the resistance of the liquid to the motion for various amplitudes and frequencies were obtained. The resistance was first represented by an equation consisting of three terms with empirical coefficients: the steady-motion drag, a term due to the 'added mass' and a term due to the history of the motion. It was found that the data could be correlated only with a large degree of scatter by this type of equation. Subsequently an attempt was made to represent the resistance by means of a single term, with an empirical coefficient C. It was found that C correlated well with the acceleration number $\dot{V}d/V^2$ and the Reynolds number Vd/ν, where $\dot{V}$, V and d are the acceleration, velocity and diameter of the sphere respectively and ν is the kinematic viscosity of the liquid. C increased with $\dot{V}d/V^2$ and decreased in the limit to the steady-motion drag coefficient C_d when $\dot{V}d/V^2$ became very small. The range of the Reynolds number in the experiments was $10^2 < Vd/\nu < 10^4$ and the range of the acceleration number was $0 \leqslant \dot{V}d/V^2 \leqslant 10{\cdot}5$.

1. Introduction

The drag on bodies, mainly spheres, in unsteady motion in fluids has been the subject of few theoretical but many experimental investigations. Early work on this subject was almost always connected with the motion of pendulums in fluids, with the object of finding the correct period of the pendulums.

Stokes (1851) showed theoretically that for a sphere oscillating linearly with small amplitude in a fluid the resistance F would be

$$F = 3\pi\nu\rho_f d[1+(pd^2/8\nu)^{\frac{1}{2}}]\,V + \tfrac{1}{2}m'[1+\tfrac{9}{2}(8\nu/pd^2)^{\frac{1}{2}}]\,\dot{V}, \tag{1}$$

where ρ_f is the density of the fluid, p is the angular frequency of the oscillations and m' is the mass of the fluid displaced by the sphere, so that for an inviscid fluid the resistance would reduce to $\frac{1}{2}m'\dot{V}$, the resistance due to the 'added mass', as deduced theoretically by Poisson (1832).

The next theoretical work in this field was done by Boussinesq (1885) and Basset (1888), who showed that for unsteady slow motion of a sphere in a fluid the solution of the Navier–Stokes equations gives

$$F = 3\pi\nu\rho_f d\,V + \tfrac{1}{2}m'\dot{V} + 6\rho_f(\pi\nu)^{\frac{1}{2}}\frac{d^2}{4}\int_0^t \frac{f(t-\tau)}{\tau^{\frac{1}{2}}}\,d\tau, \tag{2}$$

where $0 < \tau < t$ and $f(t-\tau) = \dot{V}$ at the dummy time $t-\tau$. The first term is the steady-motion drag, the second term is due to the 'added mass' and the third term is due to the history of the motion. It can be shown that substitution of a simple harmonic motion into (2) reduces it to (1).

The rest and the bulk of the work in this field has been experimental. Several of the investigators, including DuBuat (1786), Krishnaiyar (1923), Carstens (1952) and Sarpkaya (1975), confined themselves to the determination of the added-mass coefficient for spheres oscillating in liquids.

An elaborate experimental study was carried out by Odar & Hamilton (1964), who modified the Boussinesq–Basset expression by introducing empirical coefficients into all three terms. They measured the added-mass and the history coefficients for a sphere oscillating with finite amplitude in a viscous liquid. They found both coefficients to be functions of the non-dimensional quantity $V^2/(\dot{V}d)$ only. However, the Reynolds number in their experiments did not exceed 62. Later, Hamilton & Lindell (1971) showed that for spheres falling under gravity the added-mass coefficient was almost always very nearly equal to the theoretical value of 0·5 for Reynolds numbers of up to 35 000. However, they assumed initially that the history coefficient was equal to its theoretical value of 6, and did not investigate the effect of acceleration on the added-mass coefficient.

Luneau (1948), Batailler (1956) and McNown & Keulegan (1959) attempted to show experimentally that the added mass could be explained physically by the wake of the body being accelerated with it. More recently, Schöneborn (1975) showed experimentally that in an oscillatory flow the drag predicted by the empirical equation formulated by Odar & Hamilton was too low when the frequency of the flow field was in the region of the natural frequency of vortex shedding. The dependence of the flow around the sphere and hence the drag on the frequency of oscillation of the flow field had been anticipated in theoretical papers by Lighthill (1954) and Houghton (1963).

In a different approach, Lunnon (1926) expressed the fluid resistance to a sphere in unsteady motion by a different relationship, derived by dimensional analysis, namely

$$F = \rho_f V^2 d^2 g_1(Vd/\nu, \dot{V}d/V^2). \tag{3}$$

He could not verify this relationship, but by plotting $F/(V^2d^2)$ against Vd he obtained lines of constant $\dot{V}$ from data he had obtained from freely falling spheres.

Iverson & Balent (1951), in experiments on disks moving in viscous fluids, Bugliarello (1956), in experiments on spheres falling in water, and Keim (1956), in experiments on cylinders rising in water, showed that the concept of a total resistance coefficient C given by

$$F = C \times \tfrac{1}{2}\rho_f |V| V \times \tfrac{1}{4}\pi d^2, \tag{4}$$

$$C = g_2\{Vd/\nu, \dot{V}d/V^2, [V/(gd)]^{\frac{1}{2}}, \text{geometry of the body}\}$$

was more practical and gave a better correlation than the added-mass coefficient.

Despite the large amount of experimental work carried out up to now on unsteady motion of spherical bodies, the results available are deficient in some aspects. Most of the workers did not consider the history term. Those that did assumed the theoretical value given by the Boussinesq–Basset expression to apply. Accordingly, they measured the added-mass coefficient only. The results obtained by Odar & Hamilton, who measured both the added-mass and the history coefficient, were, as mentioned, for Reynolds numbers up to 62 only. It appears from their results that at such low Reynolds numbers the two coefficients are dependent on the acceleration number only. Buglia-

rello's results had a lot of scatter, so that no clear conclusion could be made. It was for these reasons that the present study was undertaken, with the aim of obtaining more conclusive results at relatively high Reynolds numbers.

2. Apparatus and experimental technique

The purpose of the apparatus was to subject a sphere, fully submerged in a liquid, to simple harmonic motion of different amplitudes and frequencies and to provide a simultaneous record of both the motion of the sphere and the liquid's resistance to it. Simple harmonic motion was chosen as a convenient method of subjecting the sphere to an unsteady motion.

The apparatus is shown in figure 1. The simple harmonic motion was produced by a horizontal bar (1) pivoted on two disks rotating together at the same speed and in the same direction. A synchronous motor (6) drove one of the disks through a gear arrangement (7) connected to the disk by a flexible shaft (8). The purpose of the flexible shaft was to isolate the measuring system from the vibrations produced by the motor. The two disks rotated together as they were connected by a positive drive belt. A hollow Perspex sphere 38·04 mm in diameter was attached by a thin vertical rod 1·5 mm in diameter to a force transducer (4). This, in turn, was fixed to the lower end of a vertical rod (2) supported by two P.T.F.E. rollers (3) on the horizontal bar. The sphere was therefore subjected to the simple harmonic motion of the horizontal bar. Provisions were made to change both the amplitude and the frequency of the oscillations.

The sphere was fully submerged in a liquid filling a cubic container of inner edge 375 mm, so that the wall effect on at least the steady-motion drag was almost negligible, as demonstrated experimentally by McNown & Newlin (1951). The liquids used were water ($\rho_f = 0{\cdot}997\,\mathrm{g/cm^3}$, $\nu = 0{\cdot}918\,\mathrm{mm^2/s}$, at a temperature of 23·8 °C) and Shell diesel oil ($\rho_f = 0{\cdot}833\,\mathrm{g/cm^3}$, $\nu = 3{\cdot}68\,\mathrm{mm^2/s}$, at a temperature of 23·0 °C).

The force transducer was made of three semicircular leaves of Perspex stuck together and spaced 120° apart. Three strain gauges (Micro Measurements, 120Ω, EA-06-125BT-120) were stuck on the inner side and three more on the outer side of the leaves. Each set of three, joined in series, formed one of two adjacent sides of a Wheatstone bridge, which was excited by a 5 V d.c. signal derived from a Hewlett–Packard (7708A) recorder system. The frequency response of the recorder was 0–150 Hz. A Disa (55D26) signal conditioner was also used for the purpose of filtering out undesirable frequencies introduced into the signal by the measuring system.

Because of its geometry the transducer, in addition to measuring axial tensile and compressive forces, was also sensitive to lateral forces on the sphere. This was apparent, as will be seen below, in the force records obtained.

Before the experiments were started some preliminary tests had to be carried out on the system. The first was the calibration of the force transducer. The load and extension showed a linear relationship. The slope was found by the least-squares method to be $k = 6897\,\mathrm{N/m}$. The load and the movement of the stylus from its neutral position also showed a linear relationship. The slope was found by the least-squares method to be $a = 0{\cdot}0128\,\mathrm{N/mm}$.

A record of the vertical oscillations of the system in air was obtained and showed the natural frequency of longitudinal oscillations of the system to be about 101 Hz.

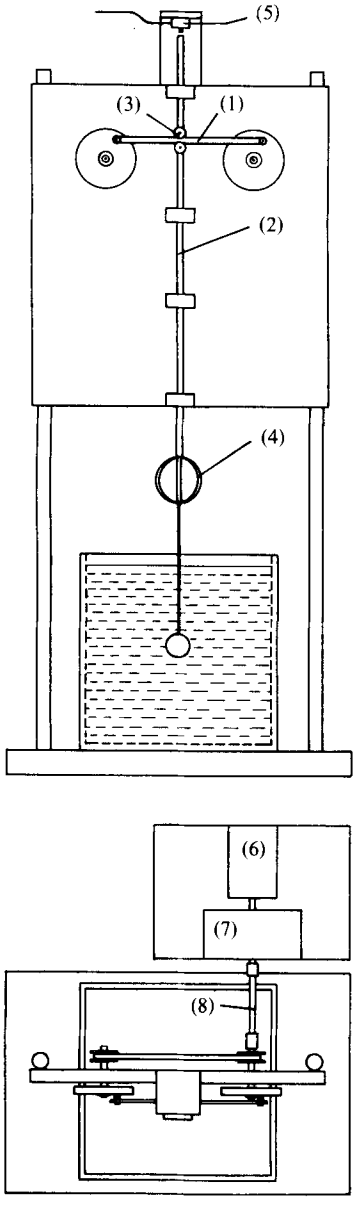

FIGURE 1. The apparatus. (1) Horizontal bar. (2) Vertical rod. (3) P.T.F.E. rollers. (4) Force transducer. (5) Microswitch. (6) Motor. (7) Gear box. (8) Flexible shaft.

From this, the effective mass M_{eff} of the transducer and the sphere combined was found to be 17·1 g under the assumption that the system was a simple spring with the sphere hanging from it. A similar record of the lateral oscillations of the system was obtained and showed the natural frequency of lateral oscillations of the system to be about 6 Hz.

Owing to the natural oscillations of the sphere, the recorder trace obtained in the experiments showed some undesirable small amplitude signals (mainly at frequencies

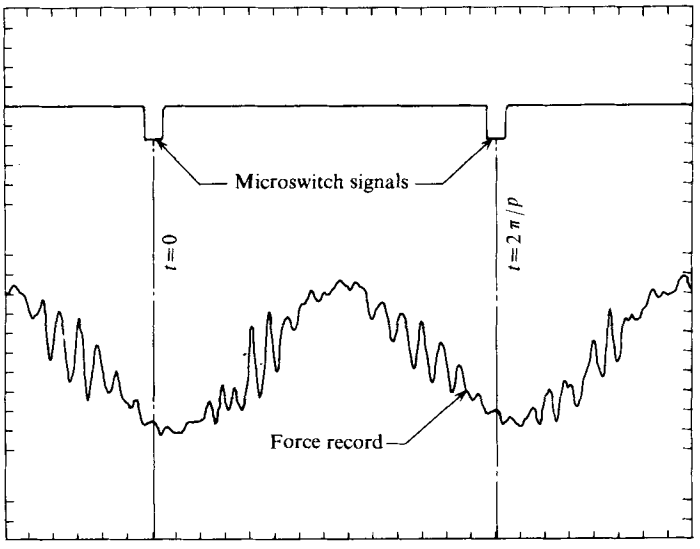

FIGURE 2. A sample of the force records. $A = 40$ mm, $p = 2{\cdot}262$ rad/s, paper speed = 25 mm/s. The liquid used was water.

of about 6 Hz and 101 Hz) superimposed on the main force record. The frequency of the simple harmonic motion in the experiments did not exceed 0·36 Hz, therefore all the oscillations above and including 10 Hz were filtered out from the signal, using the signal conditioner. (The lowest frequency that could be filtered out by the signal conditioner was 10 Hz.) Lower frequency oscillations, particularly those at 6 Hz, were eliminated by a curve-fitting procedure, as explained below.

When the preliminary tests had been completed and the system was ready, experiments were carried out to obtain records of the force on the sphere when it moved with a simple harmonic motion in the liquids mentioned above. The amplitude A of the motion was set to the values 20, 30, 40, 50 and 60 mm and its angular frequency p was set to the values 0·566, 1·131, 1·697 and 2·262 rad/s. In each of the runs a filtered record was obtained of the force on the sphere, after this had completed a few cycles of the motion. In addition, a microswitch provided a signal on the paper, alongside the force record, every time the vertical rod reached its top dead centre. This therefore gave a reference point for the displacement of the sphere. A sample of these records for $A = 40$ mm and $p = 2{\cdot}262$ rad/s is given in figure 2.

The Cartesian co-ordinates of points lying on the force records were read at equal intervals of 0·254 mm under a travelling microscope for a complete cycle, taking the microswitch signal as the starting point ($t = 0$).

On examining the form of the force records, it could be seen, as in figure 2, that apart from the small regular ripples the records were of simple harmonic form of the same angular frequency p as the motion itself. Figure 2 also shows, as is the case in all the other records, that the frequency of the ripples on the force record is about 6 Hz, the same as that for the natural lateral oscillations of the sphere. It is quite likely, therefore, that the ripples were caused by these oscillations, which were triggered and sustained by the asymmetric flow field around the sphere, as can be seen in figure 7 (a) (plate 1). In order to smooth out these small unfiltered ripples on the record curve

and to correct for the drift of the zero-amplitude line, the expression

$$b_0 + b_1 t + b_2 \sin(pt) + b_3 \cos(pt)$$

was fitted to the readings obtained with the travelling microscope by the least-squares method. After obtaining b_0, b_1, b_2 and b_3 for the particular records, the first two terms were dropped, and the force on the transducer was taken to be

$$f = a(b_2 \sin pt + b_3 \cos pt). \tag{5}$$

Re-arranging gives $f = a(b_2^2 + b_3^2)^{\frac{1}{2}} \cos[pt - \tan^{-1}(b_2/b_3)]$,

so that the force on the transducer was lagging behind the motion ($A \cos pt$) by an angle of $\tan^{-1}(b_2/b_3)$ radians. In the present investigations this angle was found to vary between 12° and 30°.

3. Theoretical analysis and calculations

The total extension z_t of the transducer could be expressed as

$$z_t = z_g + z,$$

where z_g is the extension due to the constant force $(M_{\text{eff}} - m')g$, which always acted in the same direction, and z is the extension due to the motion of the sphere in the liquid. This means that

$$z = f/k,$$

and hence

$$z = (a/k)(b_2 \sin pt + b_3 \cos pt). \tag{6}$$

If

$$y = A \cos pt + y_0 \tag{7}$$

is the displacement of a reference point on the vertical rod and x is the resulting vertical displacement of the centre of the sphere, then

$$x = y + z + L + z_g = A \cos pt + (a/k)(b_2 \sin pt + b_3 \cos pt) + L + z_g + y_0, \tag{8}$$

where y_0 and L follow from the co-ordinate system chosen as shown in figure 3.

The equation of motion of the sphere is

$$M_{\text{eff}} \ddot{x} = -k(z_g + z) - F + (M_{\text{eff}} - m')g,$$

where F is the instantaneous fluid resistance. As $kz_g = (M_{\text{eff}} - m')g$ by definition, this equation of motion can be reduced to

$$M_{\text{eff}} \ddot{x} = -kz - F,$$

from which

$$F = -M_{\text{eff}} \ddot{x} - f.$$

Substituting for $\ddot{x}$ and for f in this expression shows that the fluid resistance is

$$F = M_{\text{eff}} p^2 [A \cos pt + (a/k)(b_2 \sin pt + b_3 \cos pt)] - a(b_2 \sin pt + b_3 \cos pt), \tag{9}$$

in which all the terms are known, and therefore F can be calculated for all the points of the cycle.

It was necessary to assume an empirical expression for F and calculate the values of the empirical coefficients introduced. This was done in two ways.

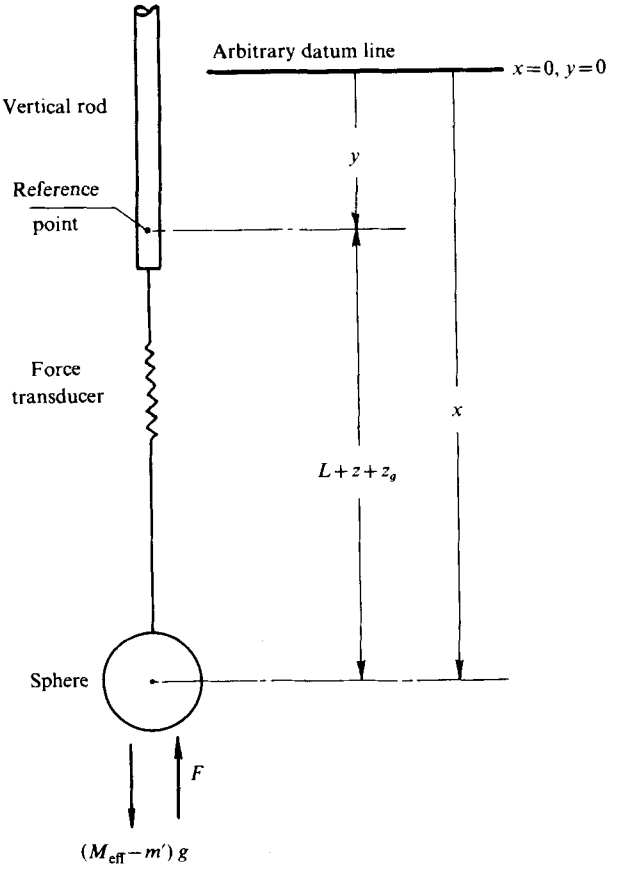

FIGURE 3. Simplified model of sphere–transducer system.

Determination of the added-mass and history coefficients

First, the method described by Odar & Hamilton was used. Empirical coefficients were introduced into the Boussinesq–Basset theoretical expression to make it applicable to motions which are not necessarily slow:

$$F = C_d \tfrac{1}{2}\rho_f |\dot{x}|\dot{x}\frac{\pi}{4}d^2 + C_m m'\ddot{x} + C_h \rho_f (\pi\nu)^{\frac{1}{2}} \frac{d^2}{4}\int_0^t \frac{\ddot{x}(t-\tau)}{\tau^{\frac{1}{2}}}\,d\tau,$$

where C_d is the steady-motion drag coefficient, C_m is the added-mass coefficient and C_h is the history coefficient. The term

$$\ddot{x}(t-\tau) = -p^2\{A\cos[p(t-\tau)] + (a/k)\sin[p(t-\tau)] + (a/k)\cos[p(t-\tau)]\}$$

is the acceleration of the sphere at the dummy time $t-\tau$.

Integration under the assumption that t is large gives

$$F = C_d\frac{\pi}{8}\rho_f d^2|\dot{x}|\dot{x} + C_m\frac{\pi}{6}\rho_f d^3\ddot{x} + C_h\frac{\pi}{4}\rho_f d^2\left(\frac{\nu}{2p}\right)^{\frac{1}{2}}(\ddot{x}+\ddot{x}'), \tag{10}$$

where

$$\ddot{x}' = -p^2[A\sin pt + (a/k)(b_3\sin pt - b_2\cos pt)]$$

is the acceleration a quarter of a cycle before the time t, with

$$\ddot{x} = -p^2[A\cos pt + (a/k)(b_2 \sin pt + b_3 \cos pt)]$$

and

$$\dot{x} = -p[A\sin pt + (a/k)(b_2 \cos pt - b_3 \sin pt)].$$

The empirical steady-motion drag coefficient C_d was obtained from the experimental data collected by Schiller & Nauman (1933), Lapple & Shepherd (1940) and Davies (1945). In order to facilitate the use of the data in the present investigations, a seventh-degree polynomial in $\log Re$ of the form

$$\log C_d = \alpha_0 + \alpha_1 \log Re + \alpha_2(\log Re)^2 + \ldots + \alpha_7(\log Re)^7 \tag{11}$$

was fitted to $\log C_d$, where

$$\alpha_0 = 1{\cdot}429, \quad \alpha_1 = -0{\cdot}8856, \quad \alpha_2 = 8{\cdot}081 \times 10^{-2}, \quad \alpha_3 = 1{\cdot}085 \times 10^{-2},$$

$$\alpha_4 = -3{\cdot}90 \times 10^{-3}, \quad \alpha_5 = 4{\cdot}31 \times 10^{-4}, \quad \alpha_6 = 2{\cdot}55 \times 10^{-4}, \quad \alpha_7 = -4{\cdot}63 \times 10^{-5}.$$

This empirical fit was applicable in the range $10^{-2} < Re < 10^5$, where $Re = Vd/\nu$.

The steady-motion drag term in (10) was therefore known. There were still two unknowns left, C_m and C_h, with only one equation available. The problem was solved by the method introduced by Odar & Hamilton. C_m was obtained at points in the cycle where the history term became zero, and similarly C_h was obtained at points in the cycle where the added-mass term became zero.

It could be shown from theoretical considerations (cf. Odar & Hamilton) or by dimensional analysis that $C_m = f_1(Re, An)$ and $C_h = f_2(Re, An)$, where in this case $Re = |\dot{x}|d/\nu$, the Reynolds number, and $An = |\ddot{x}|d/(\dot{x})^2$, the acceleration number, which is a measure of the ratio of the local acceleration term to the convective acceleration term in the Navier–Stokes equations. (An has been used by some workers in its reciprocal form.)

Therefore for each value of C_m and C_h obtained, the corresponding values of Re and An were also calculated.

Determination of the unsteady-motion drag coefficient

In the second method the concept introduced by Lunnon was used. This was simply to represent the fluid resistance by a single empirical term

$$F = C \times \tfrac{1}{2}\rho_f |\dot{x}| \dot{x} \times \tfrac{1}{4}\pi d^2,$$

where $C = f_3(Re, An)$ is the unsteady-motion drag coefficient. The Froude number was not important in this case, and the geometry factor did not apply, as only one type of object, a sphere, was used.

From the experimental data the value of C could be calculated for any point in the cycle in any of the tests. This was carried out for selected values of An.

The relationship $C = f_3(Re, An)$ was then expressed, using the available data, in the empirical form

$$C = (An + 1)^{\beta} C_d, \tag{12}$$

where C_d is the steady-motion drag coefficient, which is a function of Re only, given by (11), and $\beta = 1{\cdot}2 \pm 0{\cdot}03$, determined by the least-squares method.

The above relationship was found to give the best correlation, with the smallest standard deviation, after a trial of several other empirical forms.

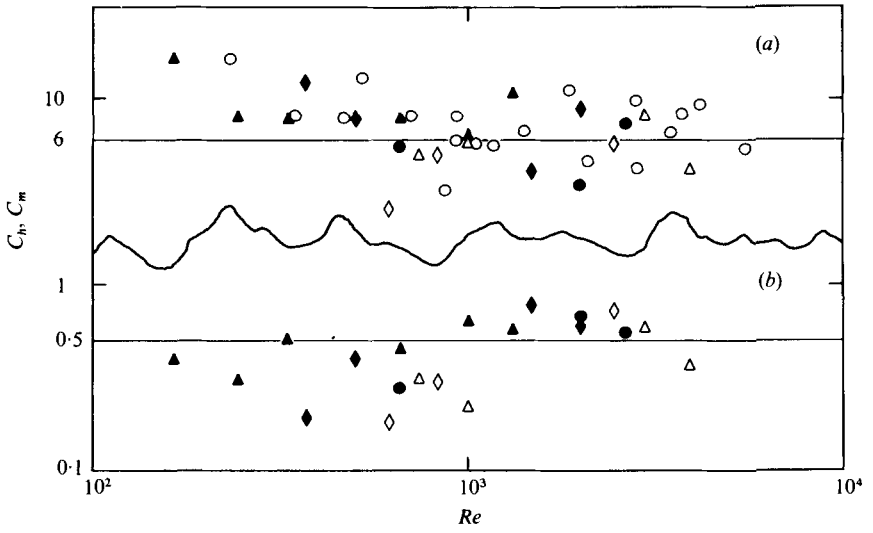

FIGURE 4. (*a*) History and (*b*) added-mass coefficient *vs.* Reynolds number. ○, $An = 0$; △, $An = 0{\cdot}89$; ◇, $An = 1{\cdot}08$; ●, $An = 1{\cdot}35$; ◆, $An = 1{\cdot}78$; ▲, $An = 2{\cdot}70$.

4. Presentation and discussion of the results

The added-mass coefficient C_m and the history coefficient C_h were calculated at certain instants in the cycle, so that the corresponding values of An were almost constant for a particular amplitude A. This made it possible to plot C_m and C_h against Re for constant values of An, as shown in figure 4.

It can be seen from this figure that in the present range of the Reynolds number ($10^2 < Re < 10^4$) there is a great degree of scatter in the plots. This can be ascribed to the form of (10), from which C_m and C_h were calculated, which tended to magnify experimental errors.

The unsteady-motion drag coefficient C was also plotted against the Reynolds number for constant values of the acceleration number as shown in figure 5. It can be seen clearly that C correlates well with both Re and An, increasing with the latter. A line showing the steady-motion drag coefficient $C_d(An = 0)$ is also included, and fits in well with the rest of the points, adding support to the present results.

A correlated form of the data for C as a function of both An and Re was obtained by statistical methods:

$$C = (An+1)^{1{\cdot}2\pm0{\cdot}03} C_d.$$

A graph of $C/(An+1)^{1{\cdot}2}$ against Re was plotted and is shown in figure 6, in which values of C_d (points at $An = 0$) are again shown as a line.

As will be seen from this figure, this type of empirical expression gives a reasonably good correlation except at the lower Reynolds numbers. However, most of the present experimental points lie above the line which represents the steady-motion drag coefficient C_d. This might be due to the additional resistance offered by the supporting rod, though owing to its small diameter this is likely to be only a minor factor. The other likely contributory factor is the eddy motion generated in the liquid by the oscillatory motion of the sphere and the shedding of vortices. A sphere moving through

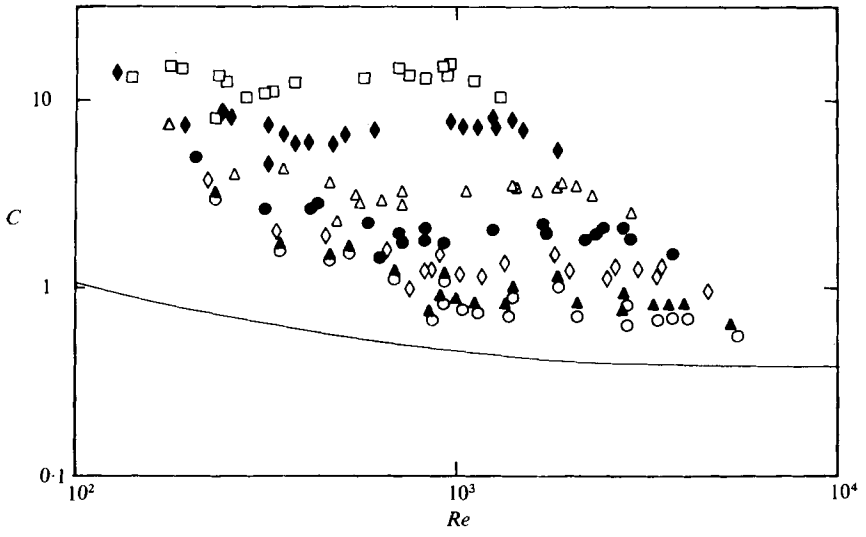

FIGURE 5. Total resistance coefficient *vs.* Reynolds number. ○, $An = 0{\cdot}1$; ▲, $An = 0{\cdot}2$; ◇, $An = 0{\cdot}5$; ●, $An = 1{\cdot}0$; △, $An = 2{\cdot}2$; ◆, $An = 5{\cdot}2$; □, $An = 10{\cdot}5$; ——, steady-motion drag curve, $An = 0$.

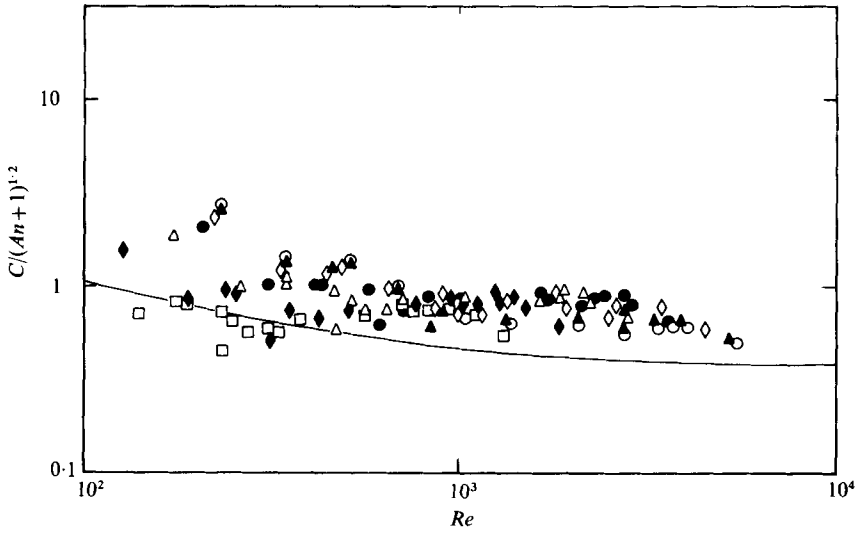

FIGURE 6. Correlated total resistance coefficient *vs.* Reynolds number. See figure 5 for notation.

such a disturbed liquid is likely to encounter greater resistance than when moving through still liquid, as is the case when the steady-motion drag coefficient is determined.

In order to get a picture of the flow pattern in the tank, a photographic flow-visualization study was undertaken. Aluminium particles were used as tracers, and the central plane of the tank, which contained the sphere, was illuminated by a parallel beam of light through a vertical slit 4 mm wide. The liquid used was water, and the amplitude and frequency of the oscillations of the sphere were varied over

the ranges covered for the drag measurements. Two photographs are shown in figure 7 (plate 1). The first, corresponding to the lowest Reynolds number in the range ($Re_{max} = 610$, where the suffix 'max' indicates the maximum value in the cycle), shows asymmetrical flow patterns, which could be produced by the shedding of vortex rings or vortex loops. Such loops have been observed by Achenbach (1974) in the wake of a sphere in steady motion. The second photograph, corresponding to the highest Reynolds number in the range ($Re_{max} = 4870$), shows an established flow pattern in the tank. In both photographs the wake can be seen to have the form of jet flow, issuing at either end of the stroke of the sphere. This wake appears to be laminar in figure 7(*a*) and turbulent in figure 7(*b*). It appears from the photographic study that the effect of the jet wake on the flow pattern in the tank increases with Re_{max} and leads to the gradual development of the two vortex rings seen in figure 7(*b*).

This limited flow-visualization study was made in order to throw some light on the nature of the flow pattern around an oscillating sphere. In view of the importance of the subject a much more comprehensive investigation would be justified.

In their work on the motion of spheres in an oscillating flow field, Baird, Senior & Thompson (1967) have found that, for values of the non-dimensional group

$$(pd/V)(A/d)^{\frac{1}{2}}$$

less than 0·07, the spheres did not suffer additional retardation due to the oscillatory nature of the motion relative to the retardation predicted by the quasi-steady equation of motion. A similar conclusion was reached by Schöneborn (1975). In the present work the range of the dimensionless number mentioned above is 0·005–0·03. It therefore follows that the experimental results on drag presented here should also be applicable to other types of motions.

5. Conclusions

It can be seen from this study that at moderate Reynolds numbers ($10^2 < Re < 10^4$) the average values of the added-mass coefficient and the history coefficient for spheres are close to their theoretical values of 0·5 and 6 respectively, as given by Boussinesq and Basset for slow motions.

The unsteady-motion drag coefficient C seems to correlate well with both the Reynolds number and the acceleration number. It decreases with the acceleration number, reducing in the limit of zero acceleration to the steady-motion drag coefficient C_d, as expected. This led to the formulation of the empirical expression for C in terms of An, C_d and Re given in (12).

The authors wish to thank Messrs J. Whiter, A. Thurston, H. Gray and A. Byrne for constructing the apparatus, and Mrs U. Harris for typing this paper.

REFERENCES

Achenbach, E. 1974 Vortex shedding from spheres. *J. Fluid Mech.* **62**, 209–221.

Baird, M. H. I., Senior, M. G. & Thompson, R. J. 1967 Terminal velocities of spherical particles in a vertically oscillating liquid. *Chem. Engng Sci.* **22**, 551–558.

Basset, A. B. 1888 On the motion of a sphere in a viscous liquid. *Phil. Trans. Roy. Soc.* A **179**, 43–63.

BATAILLER, G. 1956 Sur la similitude des champs de vitesses et des sillages courts en régimes accélérés. *C.R. Acad. Sci. Paris* **242**, 2619–2621.

BOUSSINESQ, J. 1885 Sur la résistance qu'oppose un liquide...au mouvement varié d'une sphere solide...et produits soient négligeables. *C.R. Acad. Sci. Paris* **100**, 935–937.

BUGLIARELLO, G. 1956 La resistenza al moto accelerato di sfere in acqua. *Ricerca Scientifica* **26**, 437–461.

CARSTENS, M. R. 1952 Accelerated motion of spherical particles. *Trans. Am. Geophys. Un.* **33**, 713–721.

DAVIES, C. N. 1945 Definitive equations for the fluid resistance of spheres. *Proc. Phys. Soc.* **57**, 259–270.

DUBUAT, P. L. G. 1786 *Principes d'Hydraulique*, 2nd edn, vol. 2, pp. 226–259, Paris: De L'imprimerie de Monsieur.

HAMILTON, W. S. & LINDELL, J. E. 1971 Fluid force analysis and accelerating sphere tests. *Proc. A.S.C.E.* **97** (HY6), 805–817.

HOUGHTON, C. 1963 The behaviour of particles in a sinusoidal velocity field. *Proc. Roy. Soc.* A **272**, 33–43.

IVERSEN, H. W. & BALENT, R. 1951 A correlating modulus for fluid resistance in accelerated motion. *J. Appl. Phys.* **22**, 324–328.

KEIM, S. R. 1956 Fluid resistance to accelerated cylinders. *Proc. A.S.C.E.* **82** (HY6), 1–14.

KRISHNAIYAR, N. C. 1923 An experimental determination of the inertia of a sphere vibrating in a liquid. *Phil. Mag. Ser.* 6, **46**, 1049–1053.

LAPPLE, C. E. & SHEPHERD, C. B. 1940 Calculation of particle trajectories. *Indust. Engng Chem.* **32**, 605–617.

LIGHTHILL, M. J. 1954 The response of laminar skin friction and heat transfer to fluctuations in the stream velocity. *Proc. Roy. Soc.* A **224**, 1–23.

LUNEAU, J. 1948 Sur l'effet d'inertie des sillages de corps se déplaceant dans un fluide d'un mouvement uniformément accéléré. *C.R. Acad. Sci. Paris* **227**, 823–825.

LUNNON, R. G. 1926 Fluid resistance to moving spheres. *Proc. Roy. Soc.* A **110**, 302–326.

MCNOWN, J. S. & KEULEGAN, G. H. 1959 Vortex formation and resistance in periodic motion. *Proc. A.S.C.E.* **85** (EM1), 1–6.

MCNOWN, J. S. & NEWLIN, J. J. 1951 Drag of spheres within cylindrical boundaries. *Proc. 1st U.S. Nat. Cong. Appl. Mech.* pp. 801–806.

ODAR, F. & HAMILTON, W. S. 1964 Forces on a sphere accelerating in a viscous fluid. *J. Fluid Mech.* **18**, 302–314.

POISSON, S. D. 1832 Sur les mouvements simultanés d'un pendule et de l'air environnant. *Mém. Acad. Sci. Paris* **11**, *521–582.*

SARPKAYA, T. 1975 Forces on cylinders and spheres in a sinusoidally oscillating fluid. *J. Appl. Mech., Trans A.S.M.E.* E **42**, 32–37.

SCHILLER, L. & NAUMAN, A. 1933 Uber die grundlegenden Berechnungen bei der Schwerkraftaufbereitung. *Z. Ver. dsche. Ing.* **77**, 318–320.

SCHÖNEBORN, P.-R. 1975 Bewegung einzelner Partikeln im instationären Strömungsfeld. *Chem. Ing. Tech.* **47**, 305.

STOKES, G. G. 1851 On the effect of the internal friction of fluids on the motion of pendulums. *Trans. Camb. Phil. Soc.* **9**, 8–106.

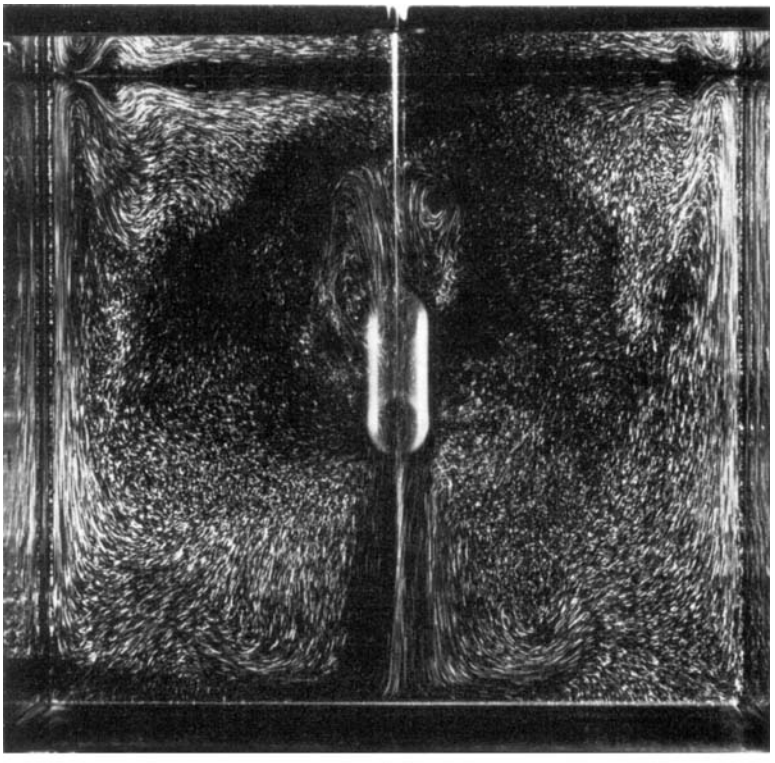

(*a*)

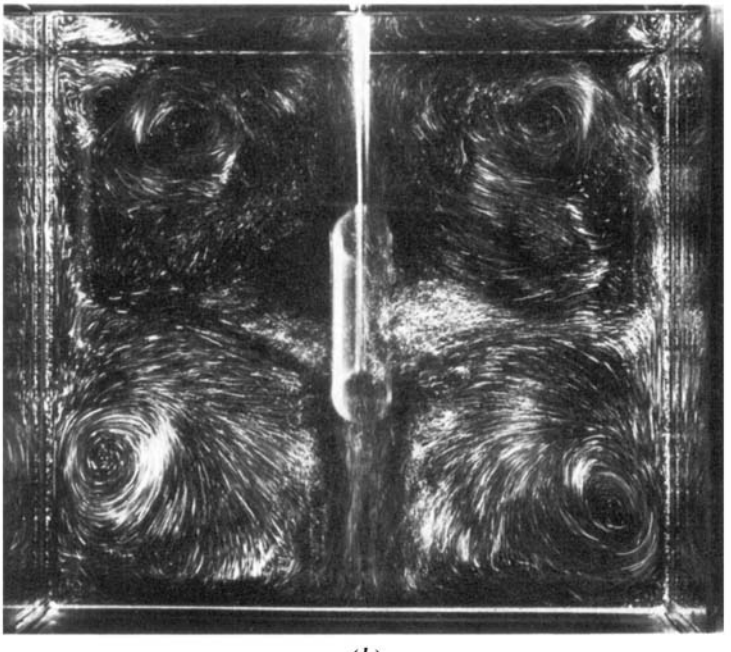

(*b*)

FIGURE 7. The flow pattern in the tank. (*a*) $A = 30$ mm, $p = 0{\cdot}09$ Hz, $Re_{\max} = 610$, exposure time = 10 s. (*b*) $A = 60$ mm, $p = 0{\cdot}36$ Hz, $Re_{\max} = 4870$, exposure time = 1 s.